수중벽면 주행로봇에 대한 강인한 비선형 예측제어기 설계

Robust Nonlinear Predictive Control of Underwater Wall-Climbing Robot

박 기 용, 윤 지 섭, 박 영 수
(Ghee Yong Park, Ji Sup Yoon and Young Soo Park)

요 약 : 본 논문에서는 강인한 비선형 예측제어기를 개발하여 연구용 원자로 벽면검사를 위한 수중로봇에 적용하여 보았다. 비선형 예측제어기는 먼저 적절한 함수 확장을 이용하여 시스템의 미래 출력 값을 예측하고, 예측값과 설정치와의 차이를 최소화시키는 제어입력을 구하여 시스템에 인가한다. 이러한 제어기에 의한 폐회로 동특성은 목적함수가 상태변수로 이루어진 경우는 항상 안정한 특성을 보이고 목적함수가 출력변수으로 이루어진 경우는 상대 계수가 4이하인 경우에 안정한 특성을 보인다. 이 제어기는 기존의 비선형 제어기가 적용 불가능한 시스템에도 적용 가능한 장점을 가지고 있다. 시스템의 불확실성이 큰 경우, 제어 안정도 및 제어 성능을 향상시키기 위하여 감독제어를 비선형 예측제어기에 포함시켰다. 이러한 제어기를 수중 벽면 주행로봇에 대한 모사실험에 적용한 결과 제어기의 강인함과 제어 성능 향상을 볼 수 있었다.

Keywords : nonlinear predictive control, supervisory control, underwater wall-climbing robot

I. Introduction

As the nuclear research reactor, TRIGA MARK III, is obsolesced and life-ended, nuclear reactor and other facilities are to be decommissioned and dismantled[1]. In the TRIGA MARK III, the radiation is emitted from the reactor core surrounded by the water-filled reactor pool (7.62×3.04×7.62m) and the inner wall of the reactor pool is contaminated by the irradiation during rector operations. The inspection of the contaminated level of inner wall surface is, therefore, the first step in decommissioning process. For performing the inspection tasks under such a hazardous environment, an underwater wall-climbing robot(UWR) is developed[2] and this robot can navigate autonomously along the surface of inner wall while inspecting the contaminated level with the radiation detector installed within the robot. The conceptual inspection procedure of UWR in TRIGA MARK III is shown in Fig. 1.

For underwater robotic vehicles(URVs), conventional control methods developed based on linear systems are not effective because of nonlinear and uncertain factors such that the vehicle has nonlinear dynamic behavior, hydrodynamics of the vehicle are poorly known and may vary with relative vehicle velocity to fluid motion, a variety of unmeasurable disturbances are present due to multi-directional currents, and the centers of gravity and buoyance may vary during operation. Nonlinear feedback control methods[3-5] were developed and have shown the robust tracking performance under parameter uncertainty. As more efficient and reliable countermove, the intelligent controller with learning capability may be a good choice for controlling URVs under uncertain operating situations such as exploration under the sea, etc. Learning control method by Yuh[6] was applied to a URV and showed good control performance.

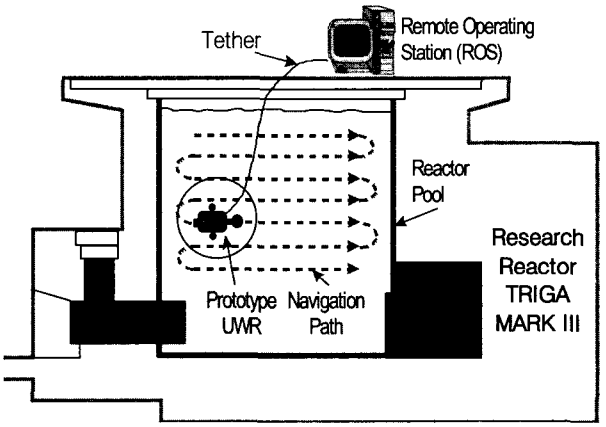

Fig. 1. Inspection procedure of UWR in TRIGA MARK III.

In this paper, a robust nonlinear predictive controller(RNPC) is developed for the motion control of UWR whose parameters and actuator dynamics vary according to operating conditions. This controller has the globally stable property under a class of uncertainty and shows good control performance.

II. Underwater wall-climbing robot for inspection

The overall operating system of UWR in the nuclear research reactor is divided into two units: the Remote Operating Station(ROS) and the UWR[2]. The ROS monitors the UWR's current status and working environment, and commands the moving path to UWR. It also receives and analyzes the inspection information transferred from UWR via

접수일자 : 1998. 1. 19., 수정완료 : 1998. 7. 10.
박기용, 윤지섭, 박영수 : 한국원자력 연구소

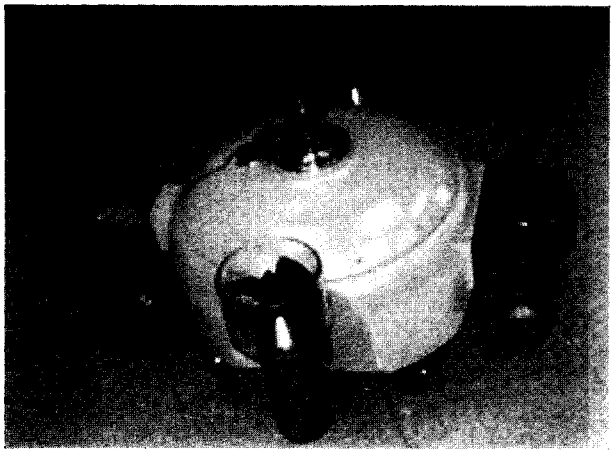

Fig. 2. Underwater wall-climbing robot.

tether which includes a communication line. UWR receives the command and power signals from ROS and performs the inspection tasks moving on the wall surface autonomously by incorporating control systems, various sensors, and actuators. As can be seen in Fig. 2, UWR has five thrusters driven by propeller. A main thruster is installed in the back of UWR and enables UWR to move forward and backward directions. Two thrusters are equipped in the front and rear positions of the UWR for rotation and position recovery. The rest two are put in both sides of UWR for adhering the UWR onto the vertical wall surface. The UWR has various sensors such as inclinometers, a laser localizer, and ultrasonic sensors. It can acquire its absolute position and deviation from moving path by inclinometers and laser localizer[2] and identify the obstacle existence by ultrasonic sensors. Using a radiation detector equipped within the UWR body, the radiation inspection tasks are performed moving along the prescribed path on the wall surface. A CCD camera and lamps are installed in front of UWR and these sensors provide the necessary information to the monitoring of ROS. The control systems are installed within the inner box of UWR for double protection of water leakage. The detailed specifications of the UWR is presented in Table 1.

The dynamic motions of UWR during inspection tasks on the wall are divided into two motion types: translational motion along and turning/rotational motion on the vertical wall. In this paper, the translational motion is only considered and is represented as follows[3][6][7]

$$M\ddot{x}(t) + C_D\dot{x}(t)|\dot{x}(t)| = F_T(t) \tag{1}$$

where x is vehicle position, t means time, M is total mass which is sum of vehicle mass and added mass[7], C_D drag coefficient, and F_T thruster force. Thruster dynamics usually affect the vehicle dynamics especially at low velocity and its dynamic characteristic is highly nonlinear. Thruster dynamic system is divided into two types; the torque-controlled thruster system and the velocity-controlled thruster system[3][6][7].

Table 1. Specifications of UWR.

Length of UWR	750 mm
Width of UWR	550 mm
Height of UWR	300 mm
Main Hull Length	500 mm
Main Hull Width	450 mm
Length of Thruster	300 mm
Diameter of Thruster	80 mm
No. of Thruster	5 EA
Material	Aluminium, Acryl
Weight in Air	47 kg
Weight in Water	0 kg
Tether Length	25 m
Tether Diameter	22 mm
No. of Wheel	4 EA
CCD Camera	1 EA
Lamp	2 EA
Laser Localizer	1 EA
Inclinometer	2 EA
Radiation Detector	1 EA
Ultrasonic Sensor	5 EA

The torque-controlled thruster system has a linear steady-state relationship between torque and thruster force, but its time constant depends on the propeller angular velocity. At high velocity, thruster dynamics can be ignored since the associated time constant is much smaller than that of vehicle dynamics. At low velocity, however, the effect of thruster dynamics on the overall vehicle dynamics becomes significant. Torque-controlled thruster dynamics are described as

$$\dot{\Omega}(t) = \beta u(t) - \alpha\Omega(t)|\Omega(t)| \tag{2a}$$

$$F_T(t) = C_T\Omega(t)|\Omega(t)| \tag{2b}$$

where Ω is the propeller angular velocity, u is the control input, α and β are constant parameters, and C_T is a proportionality constant.

The velocity-controlled thruster dynamics usually have a much smaller time constant than the vehicle dynamics and therefore, the thruster dynamics can be ignored in the vehicle control system design. However, a nonlinear relationship exists between the propeller angular velocity and the thruster force. Velocity-controlled thruster dynamics are expressed as

$$T_v\dot{\Omega}(t) + \Omega(t) = u_s(t) \tag{3a}$$

$$F_T(t) = C_T\Omega(t)|\Omega(t)| \tag{3b}$$

where T_v is a time constant and u_s is a servo control input representing a reference angular velocity. The dynamics of servo velocity control loop as in (3a) are much faster than that of the vehicle. Thruster force F_T is proportional to the square of the angular velocity as can be seen in (2b) and (3b). The proportionality constant C_T in (2b) and (3b) is unknown and changes for forward and backward motions due to the thruster configuration. The value of C_T is to be obtained experimentally through characteristic test of thruster dynamics. In this UWR, the velocity-controlled thruster systems were established and hence, (1) and (3) are used in the control system design.

III. Robust nonlinear predictive controller for UWR

The concept of predictive control was introduced in the late 70s[8] and has received great attention during 20 years. Predictive control has a strategy such that at current time, forecast the process outputs over a long range time horizon, set up the several control scenarios that drive the future plant responses to track the reference responses, and select the best candidate as a control action and apply only present control to the plant. Predictive control has shown good control results for the systems with variable parameters, variable dead time, and model order change[9-11]. Most of predictive control researches have, however, been developed based on the linear systems[12]. Lu[13] extended the predictive control concept to continuous nonlinear control system and evaluated the closed-loop stability and robustness. He also showed one useful property of NPC such that the system where existing nonlinear feedback controls are not configured can be dealt with this controller.

The predictive control concept of nonlinear systems is similar to that of existing predictive controllers based on linear systems, i.e., control system predicts the future response of the system based on the prediction model obtained from appropriate functional expansions and then, computes the control law minimizing the local difference between the predicted and desired responses.

The UWR dynamic equation as represented in (1) is rewritten as follows

$$\dot{x} = f(\boldsymbol{x}) + gu \tag{4a}$$

$$y = x \tag{4b}$$

where $\boldsymbol{x}$ is a state vector as $\boldsymbol{x}=[x\ \dot{x}]^T$, f is the nonlinear function as $f(\boldsymbol{x}) = -(C_D/M)\dot{x}|\dot{x}|$, g is the input gain with positive sign defined as $g = C_T/M$, the control input u is defined as $u=\Omega|\Omega|$, and y is the output measured by sensors. In (4), $x \in M$ ($\subset R^n, n=2$) which is some connected set containing the origin and $u \in U (\subset R^m, m=1)$ which is a compact set which defines the admissible control inputs. The functions f and g are considered to be smooth with respect to their arguments in M and also g is bounded away from zero. Then, the following assumption for system model in Eq.(4a) is introduced.

Assumption 1 : For any $u \in U$ and finite intial condition, the state trajectories are uniformly bounded for all $t \in [0, T]$.

For a small h, a future output state $x(t+h)$ can be expanded by Taylor series[13] as

$$x(t+h) = x(t) + h\dot{x}(t) + \frac{h^2}{2}\ddot{x}(t)\cdots. \tag{5}$$

In (5), $x(t+h)$ is now approximated by expanding the series to the order of the system, in this case, the system order is 2. Then, the highest order differentiation term in right hand side is replaced by the dynamic equation as in (4a) and the resulting expression is as follows

$$x(t+h) \cong x(t) + h\dot{x}(t) + \frac{h^2}{2}(f+gu). \tag{6}$$

For the validation of Taylor series, the prediction time interval, h, should be small but, as will be seen below, this value need not to be small in the formulation of control input[13]. The prediction time interval has a role of tuning parameter which adjusts the closed loop dynamics and also has that of controller gain.

At this point, we make the following assumption.

Assumption 2 : If $\boldsymbol{x}_d(t)=[x_d(t)\ \dot{x}_d(t)]^T$ is a reference state, then $\boldsymbol{x}_d(t)$ satisfies the system in (4a) with some bounded control $u^*(t) \in U$ for all $t \in [0, T]$ such as

$$\dot{x}_d = f(\boldsymbol{x}_d) + g\,u^*.$$

Then, the future reference output trajectory $x_d(t+h)$ can be expanded as

$$x_d(t+h) = x_d(t) + h\,\dot{x}_d(t) + \frac{h^2}{2}\ddot{x}_d(t). \tag{7}$$

Control objective to be minimized by the feedback control u(t) is as follows

$$J(h,t) = \frac{1}{2}\{(x(t+h) - x_d(t+h))^2 + \lambda\, u(t)^2\} \tag{8}$$

where λ is an weighting factor penalizing the control input variation. In the implementation of NPC, λ is usually set to zero.

The optimal value of u(t) minimizing the control objective of (8) should satisfy the following condition,

$$\frac{\partial J(h,t)}{\partial u(t)} = 0. \tag{9}$$

By manipulating (9) with (6) and (8), the control input u(t) is obtained as follows

$$u(t)=-\frac{\frac{h^2}{2}g}{\left(\frac{h^2}{2}g\right)^2+\lambda}\left[x(t)+h\dot{x}(t)+\frac{h^2}{2}f - x_d(t+h)\right]. \quad (10)$$

When (7) is substituted to (10), the control law is rewritten as follows

$$u(t)=-\frac{\frac{h^2}{2}g}{\left(\frac{h^2}{2}g\right)^2+\lambda}\left[e(t)+h\dot{e}(t)+\frac{h^2}{2}f - \frac{h^2}{2}\ddot{x}_d(t)\right] \quad (11)$$

where e and $\dot{e}$ are error and error rate, respectively and they are defined as $e(t)=x(t)-x_d(t)$ and

$$\dot{e}(t)=\dot{x}(t)-\dot{x}_d(t).$$

When λ is zero, the first term in right hand side of (11) can simply be $-\frac{2}{h^2}\frac{1}{g}$, and the prediction time interval h now becomes the controller gain. If h decreases, the overall controller gain increases and a large control input is produced for a small tracking error. Otherwise, if h increases, the case is reversed.

If the system functions f and g are known exactly, the error dynamics obtained by inserting (11) with λ =0 into (4a) is expressed as follows

$$\ddot{e}(t)+\frac{2}{h}\dot{e}(t)+\frac{2}{h^2}e(t)=0. \quad (12)$$

As can be seen in (12), the prediction time interval is now in charge of the error dynamics. Because h is always positive($0\le h<\infty$), the error dynamics is stable and converges to zero as $t\to\infty$, while error dynamics have always the damping ratio of 0.707 regardless of the value of h. As h is smaller, the characteristic poles of error dynamics are going to farther left side in the Laplace domain and hence, the speed of error convergence is being more increased. However, the controller gain increases as h decreases and hence, the large control input variations occur. This may generate unnecessary control input oscillations which result in large power consumption of actuator system. Therefore, the proper value of prediction time interval is to be selected from the consideration of both conflicting conditions.

When the parameter uncertainty exists in the system functions, the error dynamics have a slightly different form. In this case, we do not know f and g but the estimated functions, $\hat{f}$ and $\hat{g}$. Then, the control input $\hat{u}(t)$ based on $\hat{f}$ and $\hat{g}$ with λ=0 is

$$\hat{u}(t)=-\frac{1}{\frac{h^2}{2}\hat{g}}\left[e(t)+h\dot{e}(t)+\frac{h^2}{2}\hat{f}-\frac{h^2}{2}\ddot{x}_d\right] \quad (13)$$

The plant dynamic equation with parameter uncertainty may be represented as

$$\ddot{x}(t)=f+gu=(\hat{f}+\Delta f)+(\hat{g}+\Delta g)u = \hat{f}+\hat{g}u+d(t) \quad (14)$$

where $d(t)=\Delta f+\Delta g u(t)$ is the modeling error due to parameter uncertainty. Substituting (13) into (14) makes the error dynamics become

$$\ddot{e}(t)+\frac{2}{h}\dot{e}(t)+\frac{2}{h^2}e(t)=d(t). \quad (15)$$

Comparing (15) with (12), the error can not converge to zero when parameter uncertainty exists, but is bounded (by Assumption 1), and the tracking performance is degraded according to the magnitude of uncertainty $d(t)$.

In order to cope with uncertainty problem, instead of trying to know the exact form of f and g, we estimate the uncertainty bounds F and β for f and g, respectively such as

$$|f-\hat{f}|\le F, \quad \forall t \quad (16a)$$

$$\beta^{-1}\le\frac{\hat{g}}{g}\le\beta, \quad \forall t \quad (16b)$$

where $\hat{g}=\sqrt{g_{\max}\,g_{\min}}$ and $\beta=\sqrt{g_{\max}/g_{\min}}$ and the control input is modified so that u is sum of two controls such as

$$u(t)=\hat{u}_c(t)+u_s(t) \quad (17)$$

where $\hat{u}_c$ is the control input based on $\hat{f}$ and $\hat{g}$ as in (13) and u_s is called the supervisory control.

Let u_c^* be the control input when f and g are known exactly and this is the same form as in (11). When the control input u in (17) with both adding and subtracting the control input u_c^* is inserted to (4a), then the error dynamics become

$$\ddot{e}(t)+\frac{2}{h}\dot{e}(t)+\frac{2}{h^2}e(t)=g(\hat{u}_c(t)-u_c^*(t)+u_s(t)). \quad (18)$$

(18) can be expressed by a canonical vector form as

$$\dot{\boldsymbol{e}}=\Lambda\boldsymbol{e}+\boldsymbol{b}(\hat{u}_c-u_c^*+u_s) \quad (19)$$

where $\boldsymbol{e}=[e\ \dot{e}]^T$, $\boldsymbol{b}=[0\ \ g]^T$, and

$$\Lambda=\begin{pmatrix}0 & 1\\ -\frac{2}{h^2} & -\frac{2}{h}\end{pmatrix}.$$

Define the Lyapunov function candidate such as

$$V=\frac{1}{2}\boldsymbol{e}^T P\boldsymbol{e},\ P=P^T>0 \quad (20a)$$

and the matrix P satisfies the following condition

$$\Lambda^T P+P\Lambda=-Q\ ,\ Q>0. \quad (20b)$$

Now the task is to find u_s such that $\dot{V}\le 0$. By differentiating the (20a) with respect to time and by use of (20b), $\dot{V}$ is represented as

$$\dot{V}=-\frac{1}{2}\boldsymbol{e}^T Q\boldsymbol{e}+\boldsymbol{e}^T P\boldsymbol{b}(\hat{u}_c-u_c^*)+\boldsymbol{e}^T P\boldsymbol{b}u_s. \quad (21)$$

In (21), the term, $\hat{u}_c - u_c^*$, can be represented, by use of (11) with λ=0 and (13) , as follows

$$\hat{u}_c - u_c^* = -\frac{1}{\frac{h^2}{2}\hat{g}}\left\{\left(1-\frac{\hat{g}}{g}\right)[e(t)+h\dot{e}(t) - \frac{h^2}{2}\ddot{x}_d(t)]\right\} + \left(\frac{f}{g}-\frac{\hat{f}}{\hat{g}}\right). \quad (22)$$

The last term in right hand side of (22) is expressed as

$$\frac{f}{g}-\frac{\hat{f}}{\hat{g}} = -\frac{1}{\hat{g}}\left(\hat{f}-\frac{\hat{g}}{g}f\right)$$
$$= -\frac{1}{\hat{g}}\left(1-\frac{\hat{g}}{g}\right)\hat{f} + \frac{1}{\hat{g}}\frac{\hat{g}}{g}(f-\hat{f}). \quad (23)$$

In the above equations, f can be expressed as $\hat{f}+(f-\hat{f})$ and thereby, (23) can be made.

The magnitude of (22) can be bounded as

$$|\hat{u}_c - u_c^*| \le |\tilde{u}_c|_{\lim} \quad (24)$$

where $|\tilde{u}_c|_{\lim} = \frac{1}{\frac{h^2}{2}\hat{g}}\{(1-\beta^{-1})|e(t)+h\dot{e}(t) - \frac{h^2}{2}\ddot{x}_d(t)|\} + \frac{1}{\hat{g}}(1-\beta^{-1})|\hat{f}| + \frac{1}{\hat{g}}\beta F$.

With (24), the following inequality for $\dot{V}$ can be satisfied,

$$\dot{V} \le -\frac{1}{2}\boldsymbol{e}^T\boldsymbol{Q}\boldsymbol{e} + |\boldsymbol{e}^T\boldsymbol{P}\boldsymbol{b}|\,|\tilde{u}_c|_{\lim} + \boldsymbol{e}^T\boldsymbol{P}\boldsymbol{b}\,u_s. \quad (25)$$

If we select u_s such that

$$u_s = -sgn(\boldsymbol{e}^T\boldsymbol{P}\boldsymbol{b})\,|\tilde{u}_c|_{\lim} \quad (26)$$

where the function $sgn(s)$ is 1 when $s>0$ and is -1 when $s<0$. The resulting equation of time derivative of V with (25) and (26) becomes

$$\dot{V} \le -\frac{1}{2}\boldsymbol{e}^T\boldsymbol{Q}\boldsymbol{e}. \quad (27)$$

Since $\boldsymbol{Q}$ is positive definite, $\dot{V}$ always has a negative or zero value, and this means the Lyapunov function V in (20a) is a non-increasing function. Hence, $\boldsymbol{e}$ is uniformly bounded if initial error is bounded and this means $\boldsymbol{e} \in L_\infty$. From (26) and (24), u_s is uniformly bounded because $\hat{f}$, $\hat{g}$, $\ddot{x}_d$, and $\boldsymbol{e}$ are finite. The boundedness of f and g are deduced easily from assumption 1 with smoothness of f and g. $\hat{u}_c$ and u_c^* are also finite by assumption 1. The $\dot{\boldsymbol{e}}$ in (19) is uniformly bounded because Λ, $\boldsymbol{e}$, $\boldsymbol{b}$, u_s, $\hat{u}_c$, and u_c^* are finite and thus $\dot{\boldsymbol{e}} \in L_\infty$. By integrating both sides of (27) from t=0 to t=∞, the following expression can be made

$$\int_0^\infty \boldsymbol{e}(\tau)^T\boldsymbol{Q}\boldsymbol{e}(\tau)\,d\tau \le 2[V(0)-V(\infty)] < \infty.$$

From the above equation, $\boldsymbol{e}$ is square integrable and hence, $\boldsymbol{e} \in L_2$. Because $\boldsymbol{e} \in L_\infty \cap L_2$ and $\dot{\boldsymbol{e}} \in L_\infty$, by the Barbalat's lemma[14], it is concluded that

$$\lim_{t\to\infty} e(t) = 0.$$

From the above result, the NPC with supervisory control drives the nonlinear system which has parameter uncertainty to be stable and also it can perform the asymptotic tracking. In the calculation of the term $\boldsymbol{e}^T\boldsymbol{P}\boldsymbol{b}$, it is not required to know the exact value of $\boldsymbol{b}$ which includes an uncertain input gain. Just knowing the sign of $\boldsymbol{b}$ is sufficient for calculating the term $\boldsymbol{e}^T\boldsymbol{P}\boldsymbol{b}$ and hence, the function sgn can be easily calculated.

As can be seen in (26), the supervisory control includes the discontinuous function. If the supervisory control can provide the discontinuous values with infinite frequency, the system controlled by (13) and (26) will, indeed, be stable and show perfect tracking. When the above control inputs are applied to the motion control of UWR as represented in (4), the control input oscillations, which are so called control chattering, are appeared due to the sampling time which delays the infinite-frequency change of discontinuous function. This oscillation is a serious problem in the control system implementation because it may induce some fatal effects such as excitation of unmodeled dynamics and actuator damages[15]. In order to circumvent this problem, the supervisory control is modified as

$$u_s = \begin{cases} -sgn(s)\,|\tilde{u}_c|_{\lim} & ;|s| > s_{\lim} \\ -(s/s_{\lim})\,|\tilde{u}_c|_{\lim} & ;|s| \le s_{\lim} \end{cases}. \quad (28)$$

where $s = \boldsymbol{e}^T\boldsymbol{P}\boldsymbol{b}$ and s_{lim} is the boundary value given by a designer.

With the supervisory control of (28), the tracking error of the system with uncertainty is not driven to zero but is driven to the bounded region determined by s_{lim}.

IV. Simulations

In order to investigate the performance of robust NPC, simulation tests are performed. In the vehicle dynamics as represented in (4), the parameters M and C_D are estimated by experiment and these values are $\hat{M}$=70Kg and $\hat{C}_D$=14Ns^2/m^2. In reality, these values are varied according to the vehicle's moving condition and local fluid flow. The characteristic test for thruster dynamics is also performed and the proportionality constant is estimated from the experimental data. The estimated value of C_T is 0.00167N/s^2 for forward moving and 0.00293N/s^2 for backward moving[2].

For the representation of the effect of parameter uncertainty, the UWR's parameters are varied in this simulation such as

$$M(t) = 85 + 35\sin(|\dot{x}|t) \quad (29a)$$

$$C_D(t) = 25 + 15\sin(|\dot{x}|t) \quad (29b)$$

$$C_T(t) = 0.00167 + 0.0005\cos(t) \text{ (forward)} \quad (29c)$$

$$C_T(t) = 0.00293 + 0.0005\cos(t) \text{ (backward)} \quad (29d)$$

For the operation of UWR, the uncertainty bounds of M and C_D can be acquired from experimental and analytical analyses, but the uncertainty bound for thruster proportionality constant C_T is difficult to obtain. Therefore, the uncertainty bounds of M and C_D are incorporated into the control system design and the uncertainty of C_T is not considered by assuming the estimated value of C_T is accurate. The uncertainty bounds of F and β are calculated such as

$$\beta = \sqrt{\frac{M_{\max}}{M_{\min}}}$$

$$F = \frac{1}{\hat{M}}|\beta C_{D,\max} - \hat{C}_D|\dot{x}^2$$

where M_{max} and M_{min} are maximum and minimum values of total masses, respectively and these values are M_{max}=120 and M_{min}=50. $C_{D,max}$ is the maximum value for the variation of C_D and set to 40. When (29) are examined carefully, the variations of parameters in the vehicle and thruster systems are large. In reality, the variations of parameters are not same as in (29). In this simulation, however, the large uncertainty is configured in order to verify the efficiency of the controller.

The reference path of an UWR is prescribed as

$$x_d(t) = A\left[1 - \cos\left(\frac{2\pi}{T}t\right)\right]$$

where A=0.25m and T is 10sec. In order to protect the thruster from overload damage, the limit of angular velocity is determined from thruster characteristic test. The maximum angular velocity of propeller is limited by 70rad/s and hence, the limit of control input is $|u| \le 44100\text{rad}^2/\text{s}^2$. The limit of control input is nine times that of square of angular velocity of propeller because the angular velocity of thruster system is measured by the encoder equipped on the back of the motor and the reduction gear of ratio 3:1 is installed between the motor and the propeller[2].

For comparison of the tracking performance, PI controller, sliding mode controller[15], and robust NPC are implemented in this simulation. Fig. 3 shows the result of PI controller when the plant dynamic simulation is configured by the estimated parameter values. As can be seen in Fig. 3, the control performance of PI control is very satisfactory regardless of the nonlinear dynamic characteristics of the UWR if the plant parameter values are estimated accurately. However, when the parameter uncertainties such as (29) exist, the tracking performance is poor and unacceptable as shown in Fig. 4. In order to cope with the large parameter uncertainty, the sliding mode controller as the most compromising controller for nonlinear systems control is applied and Fig. 5 shows the result of sliding mode controller. The sliding mode controller can drive the UWR to track the reference path very well under the large parameter variation. However, the uncertainty in the thruster dynamics, which is not taken into account in the controller design, makes the sliding model controller not track the reference path perfectly. The tracking performance by the sliding mode controller is improved remarkably when it is compared with that by PI controller.

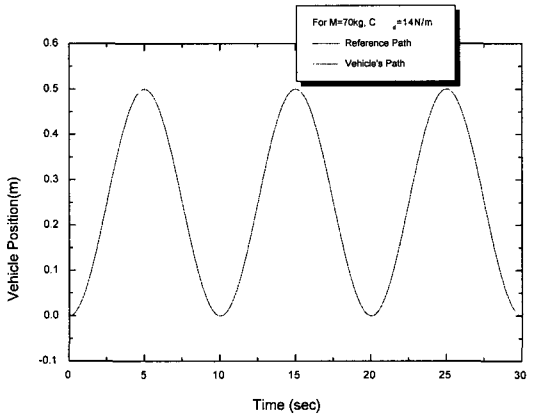

Fig. 3. Tracking performance of PI controller when the estimated parameter values are used in the simulation.

A nonlinear predictive controller without supervisory control is appled and the result of this controller is depicted in Fig. 6. The NPC controls UWR fairly well but the tracking performance is degraded when compared with sliding mode controller because the parameter uncertainty is not considered. Fig. 7 shows the result of tracking performance when the robust NPC is applied to the UWR's motion control. In Fig. 7, the results of tracking performance by the sliding mode controller and NPC are also depicted for comparison. The prediction time interval, h, is given by 1 sec. and the boundary value, s_{lim}, is set to 0.0001. In the robust NPC, the supervisory control compensates the effect of parameter uncertainty and thereby, the tracking performance is improved remarkably. It is observed that the tracking performance is improved as the boundary value is reduced, but when the boundary value is extremely small, in this simulation s_{lim}<0.000001, a few oscillation with small amplitude is appeared in control input. From the results of Fig. 7, The tracking performances of the robust NPC and the sliding mode controller are similar and satisfactory. It is said, therefore, that the

robust NPC is a good candidate in controlling the uncertain dynamic motions of UWR.

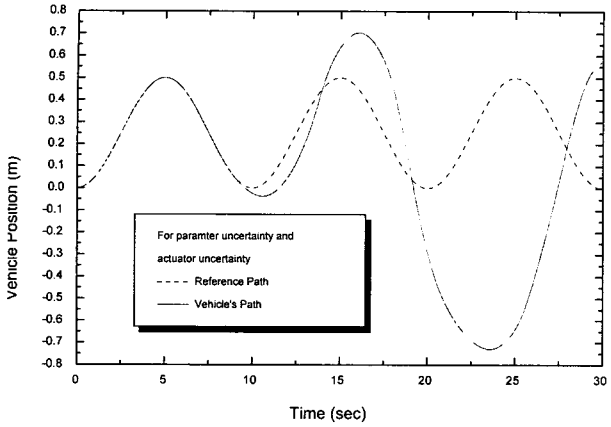

Fig. 4. Tracking performance of PI controller for a UWR with parameter uncertainty.

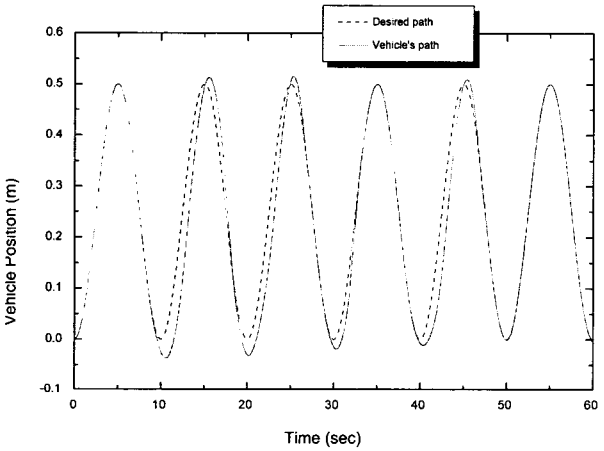

Fig. 5. Tracking performance of sliding mode controller for a UWR with parameter uncertainty.

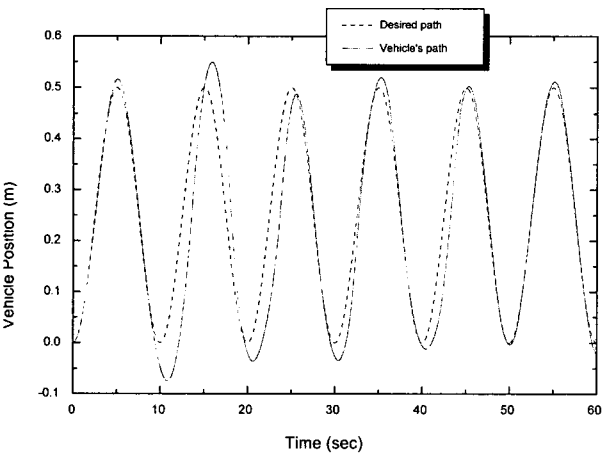

Fig. 6. Tracking performance of nonlinear predictive controller for a UWR with parameter uncertainty.

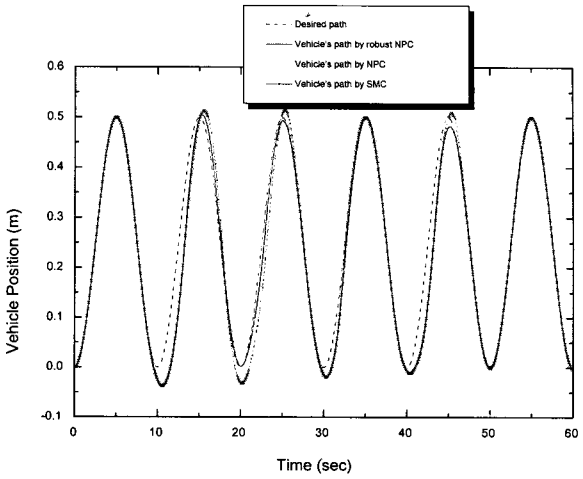

Fig. 7. Tracking performance of robust NPC for a UWR with parameter uncertainty.

V. Conclusions and further study

In this paper, a robust nonlinear predictive controller which is a nonlinear predictive controller with supervisory control is proposed and verified in the simulation experiment of an underwater wall-climbing robot developed for inspection of the contaminated wall surface in the nuclear research reactor. NPC has a general characteristic in that it can be applicable to the control problem where the recent novel approaches for nonlinear feedback control are not applicable[13]. For perfect tracking for the parameter uncertainty, the supervisory control is involved in the design of NPC. This robust controller can cope with the uncertain nonlinear system but produces the control chattering. In order to remove the control chattering, the supervisory control is smoothed out within the prescribed boundary region and thereby, tracking error is guaranteed to be uniformly bounded. Simulation results show the good tracking performance of this controller and conclude that the robust NPC is a good candidate in controlling the motion of UWR. In the further study, multidimensional tracking operations such as rotation and position recovery from external disturbances are to be accomplished with this controller and the experiment of UWR in the reactor pool will be carried out. At present time, the communication system and the structure of ROS are being constructed for experiment and the results of experiment of the UWR with this controller will be presented in the near future.

References

[1] KAERI-NEMAC/RR-176/96., *Radioactive Waste Basic Research and Development: Decontamination, Restoration, and Recycling Technology Development*, 1st Final Report, KAERI, 1996.

[2] 김병만, 김경훈, 조형석, 박영수, 윤지섭, 박기용, "수중 벽면 주행 기구의 설계," *'97 Korea Automatic Control Conference*, FA1-12-3, pp. 237-240, 1997.
[3] D. R. Yoerger, J. G. Cookie and J.-J. E. Slotine, "The influence of thruster dynamics on underwater vehicle behavior and their incorporation into control system design," *IEEE J. of Ocean Engineering*, vol. 15, no. 3, pp. 167-178, 1990.
[4] R. Cristi, F. A. Papoulis and A. J. Healy, "Adaptive sliding mode control of autonomous underwater vehicles in the dive plane," *IEEE J. of Ocean Engineering*, vol. 15, no. 3, pp. 152-160, 1990.
[5] A. J. Healy and D. Lienard, "Multivariable sliding mode control for autonomous diving and steering of unmanned underwater vehicles," *IEEE J. of Ocean Engineering*, vol. 13, no. 3, pp. 327-339, 1993.
[6] J. Yuh, "Learning control for underwater robotic vehicles," *IEEE Control Systems Magazine*, vol. 14, no. 2, pp. 39-46, 1994.
[7] J. Yuh, *Underwater Robotic Vehicles*, TSI Press, 1995.
[8] J. Richalet, et al., "Model predictive heuristic control : application to industrial processes," *Automatica*, vol. 14, no. 5, pp. 413-428, 1978.
[9] D. W. Clarke, C. Mohtad and P. S. Tuffs, "Generalized predictive control - Part I. basic algorithm," *Automatica*, vol. 23, no. 2, pp. 137-148, 1987.
[10] B. E. Ydstie, "Extended horizon adaptive control," *Proc. 9th IFAC World Congress*, Budapest, Hungary, 1984.
[11] A. R. Cauwenberghe, et al., "Self adaptive long range predictive control," *Proc. American Control Conference*, TP10, pp. 1155-1160, 1985.
[12] R. Soeterboek, *Predictive Control : A Unified Approach*, Prentice-Hall, New York, 1992.
[13] P. Lu, "Optimal predictive control of continuous nonlinear systems," *Int. J. of Control*, vol. 62, no. 3, pp. 633-649, 1995.
[14] V. M. Popov, *Hyperstability of Control Systems*, Springer-Verlag, New York, 1973.
[15] J.-J. E. Slotine and W. Li, *Applied Nonlinear Control*, Prentice Hall, 1991.

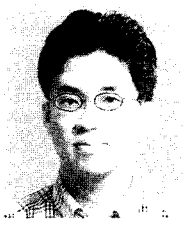

박 기 용

1990년 한양대학교 원자력공학과 졸업. 한국과학기술원 원자력공학과 석사(1992) 동대학원 박사(1986). 1996년-현재 한국원자력연구소 사용후핵연료 원격취급장치개발팀 Post- Doc. 관심분야는 지능제어, 비선형강인제어, 분산시스템제어, 시스템 모델링 및 분석.

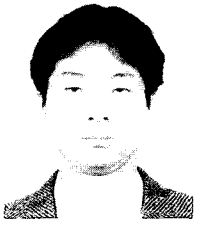

박 영 수

1986년 Georgia Institue of Technology 기계공학과 졸업. 동대학원 석사(1988). 한국과학기술원 기계공학과 박사(1996). 1987년-현재 한국원자력연구소 사용후핵연료 원격취급장치개발팀 선임연구원. 관심분야는 로봇 작업영역 해석, Task Planning, 로봇 제어, 원격로봇 시스템 설계.

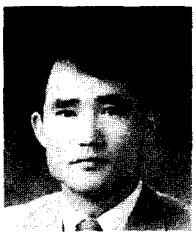

윤 지 섭

1980년 서울대학교 기계공학과 졸업. 한국과학기술원 기계공학과 석사(1982) 동대학원 박사(1987). 1987년-현재 한국원자력연구소 사용후핵연료 원격취급장치개발팀 책임연구원/팀장. 관심분야는 산업공정 원격취급기술, 생산자동화 및 계측제어, 로봇 및 센서 적용 기술.